# Coupled-Channel Analysis of the $\chi_{c1}(3872)$ Line Shape with BESIII Data

M. Ablikim *et al.*[*]
(BESIII Collaboration)

(Received 5 September 2023; revised 3 January 2024; accepted 11 March 2024; published 12 April 2024)

We perform a study of the $\chi_{c1}(3872)$ line shape using the data samples of $e^+e^- \to \gamma\chi_{c1}(3872)$, $\chi_{c1}(3872) \to D^0\bar{D}^0\pi^0$, and $\pi^+\pi^-J/\psi$ collected with the BESIII detector. The effects of the coupled channels and the off-shell $D^{*0}$ are included in the parametrization of the line shape. The line shape mass parameter is obtained to be $M_X = (3871.63 \pm 0.13^{+0.06}_{-0.05})$ MeV. Two poles are found on the first and second Riemann sheets corresponding to the $D^{*0}\bar{D}^0$ branch cut. The pole location on the first sheet is much closer to the $D^{*0}\bar{D}^0$ threshold than the other, and is determined to be $7.04 \pm 0.15^{+0.07}_{-0.08}$ MeV above the $D^0\bar{D}^0\pi^0$ threshold with an imaginary part $-0.19 \pm 0.08^{+0.14}_{-0.19}$ MeV.

DOI: 10.1103/PhysRevLett.132.151903

The $\chi_{c1}(3872)$ state, also known as $X(3872)$, was discovered in $B^\pm \to [\chi_{c1}(3872) \to \pi^+\pi^-J/\psi]K^\pm$ decay processes by the Belle experiment [1], and confirmed by CDF [2], D0 [3], and *BABAR* [4]. As the first candidate of an exotic charmoniumlike state, it has been studied in numerous experimental analyses over the past two decades. Along with a well-established quantum number $J^{PC} = 1^{++}$ [5], many remarkable features of the $\chi_{c1}(3872)$ have been observed, including a mass almost exactly at the $D^{*0}\bar{D}^0$ threshold, an extremely narrow width [6], and an isospin-violating decay pattern [7–9]. For the nature of the $\chi_{c1}(3872)$, many theoretical interpretations have been proposed, including a hadronic molecule [10,11], a compact tetraquark state [12], a conventional charmonium state $\chi_{c1}(2P)$ [13], a mixture of a molecule, and an excited charmonium state [14–16].

The line shape of the $\chi_{c1}(3872)$ contains essential information, since from its parameters it is possible to extract the pole locations, the effective range of the particle interaction, and the scattering length. Here, the pole of a physical state refers to the corresponding single pole of the off-shell $T$ matrix in the complex energy plane, where the amplitude becomes infinite. Recently, the LHCb experiment performed a line-shape study based on a high-statistics $\chi_{c1}(3872) \to \pi^+\pi^-J/\psi$ data sample, with both Breit-Wigner and Flatté models [17]. However, the line shapes based on these two models cannot be distinguished once the mass resolution is considered. Because of the proximity to the $D^*\bar{D}$ threshold, the line shape of the $\chi_{c1}(3872)$ in the $D^{*0}\bar{D}^0$ channel is significantly distorted, making this channel more sensitive to the behavior of the $T$ matrix. A study of $\chi_{c1}(3872) \to D^*\bar{D}$ has previously been performed by Belle [18]; however, the off-shell effect of the $D^{*0}$ was not taken into account due to a mass constraint applied to the $D^0\pi^0$ and $D^0\gamma$ systems coming from the $D^{*0}$, which forced the distribution to start from the $D^{*0}\bar{D}^0$ threshold. In the meantime, data samples of both $\chi_{c1}(3872) \to \pi^+\pi^-J/\psi$ and $\chi_{c1}(3872) \to D^0\bar{D}^0\pi^0$ channels were acquired by BESIII [19], allowing a simultaneous fit, taking into account the coupled-channel effect and the width of the $D^{*0}$, which can improve the $\chi_{c1}(3872)$ line-shape measurement.

In this Letter, we present a study of the $\chi_{c1}(3872)$ line shape using $e^+e^-$ annihilation data collected with the BESIII detector at center-of-mass energies ranging from 4.178 to 4.278 GeV, already used in previous $\chi_{c1}(3872)$ studies [19]. The total integrated luminosity is 9.0 fb$^{-1}$ [20,21]. The data samples used have center-of-mass energies around the $Y(4230)$ mass peak, since these energies correspond to a maximum in the $\chi_{c1}(3872)$ production cross section. The pole locations of the $\chi_{c1}(3872)$ are determined based on a simultaneous fit to the data samples of $\chi_{c1}(3872) \to D^0\bar{D}^0\pi^0$ and $\chi_{c1}(3872) \to \pi^+\pi^-J/\psi$, with the $\chi_{c1}(3872)$ produced in the $e^+e^- \to \gamma\chi_{c1}(3872)$ process. For $D^0\bar{D}^0\pi^0$ channel, $|M(D^0\pi^0) - m_{D^{*0}}| < 4\ \mathrm{MeV}/\mathrm{c}^2$ is required [19], where $m_{D^{*0}}$ is the mass of $D^{*0}$ [6]. Throughout this Letter, the charge conjugations are always included and the notations $D^{*0}\bar{D}^0$ and $D^{*+}D^-$ denote both themselves and their charge conjugations.

The parametrization scheme in this analysis is developed based on the framework described in Ref. [22], taking into account the effects of the $D^{*0}$ width. In this framework, the $\chi_{c1}(3872)$ decays into the three-body final state $D^0\bar{D}^0\pi^0$ via

---

[*] Full author list given at the end of the Letter.

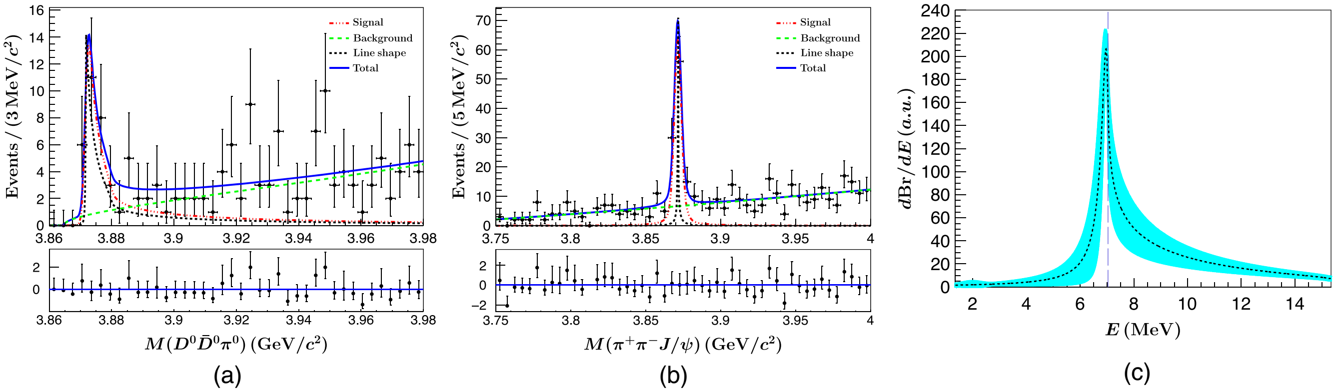

FIG. 1. Distributions of (a) $D^0\bar{D}^0\pi^0$ and (b) $\pi^+\pi^-J/\psi$ invariant mass. The black dots with error bars are the data from Ref. [19]; the blue continuous lines are the probability density functions at the best estimation; the red dotted lines are the signal shapes; the green dashed lines are the background shapes; and the black dashed lines represent the line shape without the mass resolution considered, normalized to the signal height for comparison. (c) The $\chi_{c1}(3872)$ line shape at the best estimation. Here, $d\mathrm{Br}/dE$ is $(g \times k_{\mathrm{eff}} + \Gamma_0)/|D(E)|^2$ in arbitrary units (a.u.). The cyan shaded band indicates the statistical uncertainty and the vertical dashed line indicates the position of the $D^{*0}\bar{D}^0$ threshold.

intermediate $D^{*0}\bar{D}^0$. The differential decay rate is written as

$$\frac{d\mathrm{Br}(D^0\bar{D}^0\pi^0)}{dE} = \mathcal{B}\frac{\mathrm{Br}(D^{*0} \to D^0\pi^0) \times g \times k_{\mathrm{eff}}(E)}{|D(E)|^2},$$
$$\frac{d\mathrm{Br}(\pi^+\pi^-J/\psi)}{dE} = \mathcal{B}\frac{\Gamma_{\pi^+\pi^-J/\psi}}{|D(E)|^2}, \tag{1}$$

where the denominator is

$$D(E) = E - E_X + \frac{1}{2}g[(\kappa_{\mathrm{eff}}(E) + ik_{\mathrm{eff}}(E)) + (\kappa^c_{\mathrm{eff}}(E) + ik^c_{\mathrm{eff}}(E))] + \frac{i}{2}\Gamma_0. \tag{2}$$

In the above equations, all the details of the $\chi_{c1}(3872)$ production are assumed to be absorbed in a global constant factor $\mathcal{B}$, while Br denotes the branching fractions, and $g$ denotes the effective coupling constant of the $\chi_{c1}(3872)$ to neutral and charged $D^*\bar{D}$. The energy $E$ ($E_X$) is measured with respect to the three-body $D^0\bar{D}^0\pi^0$ threshold, and is related to the invariant mass of the final states [the mass of the $\chi_{c1}(3872)$] by $M_{(X)} = m_{D^0} + m_{\bar{D}^0} + m_{\pi^0} + E_{(X)}$, where $m_{D^0}$, $m_{\bar{D}^0}$, and $m_{\pi^0}$ are the masses of $D^0$, $\overline{D^0}$, and $\pi^0$ quoted from the Particle Data Group [6]. The constant $\Gamma_0$ includes the width of all channels except $D^*\bar{D}$, and is composed of three parts: $\Gamma_0 = \Gamma_{\pi^+\pi^-J/\psi} + \Gamma_{\mathrm{known}} + \Gamma_{\mathrm{unknown}} = (1+\beta+\alpha)\Gamma_{\pi^+\pi^-J/\psi}$. Here, $\Gamma_{\pi^+\pi^-J/\psi}$, $\Gamma_{\mathrm{known}}$ and $\Gamma_{\mathrm{unknown}}$ are the partial widths of the $\pi^+\pi^-J/\psi$ channel, the other measured channels [$\gamma J/\psi$, $\gamma\psi(3686)$, $\pi^0\chi_{c1}$, and $\omega J/\psi$], and the unknown channels, respectively. Because of limited statistics, the ratio $\alpha = \Gamma_{\mathrm{unknown}}/\Gamma_{\pi^+\pi^-J/\psi}$ is fixed at 8 and the ratio $\beta = \Gamma_{\mathrm{known}}/\Gamma_{\pi^+\pi^-J/\psi}$ is fixed at 2.8, according to a global analysis of $\chi_{c1}(3872)$ decays [23]. The $\kappa^{(c)}_{\mathrm{eff}}(E)$ and $k^{(c)}_{\mathrm{eff}}(E)$ in Eq. (2) (the superscript $c$ indicates the charged $D^{*+}D^-$) are self-energy correction from $\chi_{c1}(3872) \to D^*\bar{D}$, with unstable $D^*$ [22]. The parametrization of them can be found in the Supplemental Material [24].

The expected numbers of signal events in the two decay channels, $\mu_{D^0\bar{D}^0\pi^0}$ and $\mu_{\pi^+\pi^-J/\psi}$, are related to the number of produced $e^+e^- \to \gamma\chi_{c1}(3872)$ events, $\mu^{\mathrm{prod}}_{\chi_{c1}(3872)}$, as follows:

$$\mu_{D^0\bar{D}^0\pi^0} = \epsilon_{D^0\bar{D}^0\pi^0} \times R_{D^0\bar{D}^0\pi^0} \times \mu^{\mathrm{prod}}_{\chi_{c1}(3872)},$$
$$\mu_{\pi^+\pi^-J/\psi} = \epsilon_{\pi^+\pi^-J/\psi} \times R_{\pi^+\pi^-J/\psi} \times \mu^{\mathrm{prod}}_{\chi_{c1}(3872)}. \tag{3}$$

Here, $\epsilon_{D^0\bar{D}^0\pi^0}$ ($\epsilon_{\pi^+\pi^-J/\psi}$) represents the efficiency of the $D^0\bar{D}^0\pi^0$ ($\pi^+\pi^-J/\psi$) channel multiplied by the branching fractions of the decay chains $D^0 \to K^-\pi^+$, $K^-\pi^+\pi^0$, $K^-2\pi^+\pi^-$, $\pi^0 \to \gamma\gamma$ ($J/\psi \to e^+e^-, \mu^+\mu^-$), i.e., $1.31 \times 10^{-3}$ ($3.78 \times 10^{-2}$) according to Refs. [6,9,19], while $R_{D^0\bar{D}^0\pi^0}$ ($R_{\pi^+\pi^-J/\psi}$) represents the branching fraction of $\chi_{c1}(3872) \to D^0\bar{D}^0\pi^0$ [$\chi_{c1}(3872) \to \pi^+\pi^-J/\psi$] derived from the line-shape analysis.

The mass resolutions of the two channels are studied based on Monte Carlo (MC) simulation. The MC samples are generated with zero $\chi_{c1}(3872)$ width and a series of mass values in the range of interest. For the $D^0\bar{D}^0\pi^0$ channel, the mass resolution is modeled as a Gaussian function, with a constant mean and a linear mass-dependent width. For the $\pi^+\pi^-J/\psi$ channel, the mass resolution is modeled by a Gaussian function, whose parameters are determined by the control sample $e^+e^- \to \gamma_{\mathrm{ISR}}[\psi(2S) \to \pi^+\pi^-J/\psi]$ and calculated at 3.872 GeV. The values of mass shift and resolution can be found in the Supplemental Material [24].

TABLE I. Summary of the $\chi_{c1}(3872)$ line-shape fit parameters.

| Parameter | Symbol | Value |
|---|---|---|
| Coupling constant | $g$ | Fit |
| Partial width of $\pi^+\pi^-J/\psi$ | $\Gamma_{\pi^+\pi^-J/\psi}$ | Fit |
| Physical mass of $\chi_{c1}(3872)$ | $M_X$ | Fit |
| Mass of $D^{*0}$ | ⋯ | 2.006 85 GeV |
| Width of $D^{*0}$ | ⋯ | 55.9 keV |
| Width of $D^{*\pm}$ | ⋯ | 83.4 keV |
| $\Gamma_{\text{known}}/\Gamma_{\pi^+\pi^-J/\psi}$ | $\beta$ | 2.8 |
| $\Gamma_{\text{unknown}}/\Gamma_{\pi^+\pi^-J/\psi}$ | $\alpha$ | 8 |
| Total number of $\chi_{c1}(3872)$ | $\mu^{\text{prod}}_{\chi_{c1}(3872)}$ | Fit |
| Efficiency correction[a] | $\epsilon_{D^0\bar{D}^0\pi^0}$ | $1.31\times10^{-3}$ [19] |
|  | $\epsilon_{\pi^+\pi^-J/\psi}$ | $3.78\times10^{-2}$ [9] |

[a] Multiplied with branching fractions of daughter particles' decay.

An unbinned maximum likelihood fit is performed simultaneously to the invariant mass distributions of $M(\pi^+\pi^-J/\psi)$ and $M(D^0\bar{D}^0\pi^0)$, whose parameters are summarized in Table I. In the fit, to improve the mass resolution, the variable $M(\pi^+\pi^-J/\psi) = M(\pi^+\pi^-l^+l^-) - M(l^+l^-) + m_{J/\psi}$ is used, where $l^+l^-$ stands for $e^+e^-$ or $\mu^+\mu^-$, and $m_{J/\psi}$ is the $J/\psi$ mass [6]. The signal shapes for the $D^0\bar{D}^0\pi^0$ and $\pi^+\pi^-J/\psi$ channels are modeled as their corresponding differential rates [Eq. (1)] convoluted with the resolution functions. The background shapes for the $D^0\bar{D}^0\pi^0$ and $\pi^+\pi^-J/\psi$ channels are described, respectively, by an ARGUS function [25] with threshold parameters fixed at the $D^0\bar{D}^0\pi^0$ nominal mass, and by a second order Chebyshev function. The obtained line-shape parameters are shown in Table II, and the number of produced $\chi_{c1}(3872)$ is determined to be $\mu^{\text{prod}}_{\chi_{c1}(3872)} = (9.8\pm3.9)\times10^4$. Here, the floating parameter in the fit is $\Gamma_{\pi^+\pi^-J/\psi}$ and its value is transformed into $\Gamma_0 = (1+\alpha+\beta)\Gamma_{\pi^+\pi^-J/\psi}$ throughout the Letter for convenience. The fit result is shown in Figs. 1(a) and 1(b), and the obtained $\chi_{c1}(3872)$ line shape, adding all channels together, is shown in Fig. 1(c), with a full width at half maximum (FWHM) of 0.44 MeV.

The systematic uncertainties are estimated as follows.

The uncertainty caused by the choice of the ratios $\alpha = \Gamma_{\text{unknown}}/\Gamma_{\pi^+\pi^-J/\psi}$ and $\beta = \Gamma_{\text{known}}/\Gamma_{\pi^+\pi^-J/\psi}$ is evaluated by varying $\alpha+\beta$ in the range (4.2, 21.8), according to Ref. [23].

TABLE II. The fit results of the line-shape parameters and the correlation matrix.

| Parameters | $g$ | $\Gamma_0$ (MeV) | $M_X$ (MeV) |
|---|---|---|---|
| Fit results | $0.16\pm0.10$ | $2.67\pm1.77$ | $3871.63\pm0.13$ |
| $g$ | 1.00 | 0.89 | −0.60 |
| $\Gamma_0$ |  | 1.00 | −0.29 |
| $M_X$ |  |  | 1.00 |

TABLE III. Systematic uncertainties of the line-shape parameters.

| Source | $g$ | $\Gamma_0$ (MeV) | $M_X$ (MeV) |
|---|---|---|---|
| $\alpha$ | $+1.08-0.10$ | $+6.54-0.65$ | $+0.05-0.04$ |
| $\Gamma_{D^{*0}}$ | ⋯ | $+0.05-0.07$ | ⋯ |
| Efficiency | $+0.05-0.03$ | $+0.35-0.24$ | ⋯ |
| Resolution | ⋯ | $\pm0.02$ | ⋯ |
| Background | $+0.05$ | $+0.51-0.24$ | $\pm0.01$ |
| $M(D^0)$ | ⋯ | $+0.11-0.09$ | $\pm0.03$ |
| $E_{\text{cms}}$ | $+0.29$ | $+4.57$ | $-0.01$ |
| Simulation | $\pm0.02$ | $\pm0.26$ | $\pm0.01$ |
| Sum | $+1.12-0.11$ | $+8.01-0.82$ | $+0.06-0.05$ |

The $D^{*0}$ nominal width is quoted from an evaluation based on heavy quark symmetry [26]. The corresponding uncertainty is estimated by varying the value in the range (50, 70) keV in the line-shape models, where the range is determined according to various calculations of the $D^{*0}$ width (55.9 keV in Ref. [26], 53.7 keV in Ref. [27], and 68 keV in Ref. [28]).

The relative uncertainty from the efficiency ratios of the $D^0\bar{D}^0\pi^0$ and $\pi^+\pi^-J/\psi$ decays is assigned to be 10% according to the uncorrelated uncertainties in Refs. [9,19], and is propagated to the line-shape parameters by changing the corresponding values in Eq. (3).

The discrepancy in the $D^0\bar{D}^0\pi^0$ mass resolution between MC simulation and data (referred to as Resolution” in Table III) is studied using the control sample $e^+e^- \to [D^{*0} \to D^0\pi^0]\bar{D}^0$. The discrepancy is parametrized as a Gaussian function and extracted from the distribution of $M_{\text{control}} = |2p_D + p_{\pi^0}|$, where $p_{\pi^0}$ and $p_D$ denote the four-momentum of the $\pi^0$ and of the $D^0$ decaying from $D^{*0}$, respectively. The obtained Gaussian function is convoluted additionally with the line shape for uncertainty evaluation. For the $\pi^+\pi^-J/\psi$ channel, since the MC invariant mass has been modeled to data by using the control sample, the related systematic uncertainty is treated as negligible.

For the background models (referred as “Background” in Table III), the uncertainty is evaluated by changing the ARGUS function to a third order polynomial, and changing the order of the Chebyshev function from second to third.

The uncertainty of the $D^0$ mass, 50 keV [6], is propagated to the line-shape parameters by changing the $D^0$ mass by ±50 keV in the analysis procedure.

The center-of-mass energies of the $e^+e^-$ collisions for the datasets used in this work are obtained from a measurement of di-muon events, as described in Ref. [29]. A common uncertainty of 0.8 MeV for each dataset is adopted, and it is propagated to the line-shape parameters by changing the values of the center-of-mass energies accordingly when applying the kinematic constraints in the event selection.

The uncertainties caused by MC simulation configurations (referred as "Simulation" in Table III), including the input cross sections and the generator models used in the decay chains, are evaluated as follows. For the input cross sections of $e^+e^- \to \gamma\chi_{c1}(3872)$, the measured cross sections of Ref. [9] are used, instead of using the $Y(4230)$ line shape quoted from the Particle Data Group; for the $\gamma\chi_{c1}(3872)$ angular distribution, it is changed from an E1 transition to a pure $S$ wave; the $\pi^+\pi^-$ pair in the $\pi^+\pi^- J/\psi$ channel is assumed to come from a $\rho^0$ decay, and for the $\rho J/\psi$ angular distribution from $\chi_{c1}(3872)$ the partial wave analysis result of Ref. [5] is adopted, instead of the original $S$-wave assumption.

For each of the above mentioned sources of systematic uncertainties, the largest differences caused by varying the values or modifying the inputs with respect to the nominal values are taken as systematic uncertainties, and are treated as independent. The systematic uncertainties of the line-shape parameters are summarized in Table III, where the last row is obtained by summing each term in quadrature.

The analytic structure of the amplitude and the corresponding pole locations are studied by extending the energy $E$ from the real axis to the whole complex plane. According to the simplified form in the Supplemental Material [24], there are two Riemann sheets with respect to the $D^{*0}\bar{D}^0$ threshold, defined by the sign of the $D^{*0}\bar{D}^0$ self-energy term

$$\text{Sheet I:}\quad -g\sqrt{-2\left(E - E_R + \frac{i\Gamma_{D^{*0}}}{2}\right)} + i\Gamma_0,$$

$$\text{Sheet II:}\quad +g\sqrt{-2\left(E - E_R + \frac{i\Gamma_{D^{*0}}}{2}\right)} + i\Gamma_0. \qquad (4)$$

The numerical results on the pole locations are obtained using a complex roots finding algorithm [30]. The pole locations are visualized by plotting the phase of the amplitude, as shown in Fig. 2, where the phase is indefinite around the poles and discontinuous across the branch cut. With the nominal line-shape parameters, two poles are found: one is on Sheet I, denoted as $E_{\mathrm{I}}$, while the other is on Sheet II, denoted as $E_{\mathrm{II}}$. As shown in Fig. 2, the location of $E_{\mathrm{I}}$ is much closer to the $D^{*0}\bar{D}^0$ threshold than $E_{\mathrm{II}}$.

The pole locations on the $k$ plane are also investigated. The momentum $k$ is defined by $k = \sqrt{2\mu_p}\sqrt{E - E_R + (i\Gamma_{D^{*0}}/2)}$, where $\mu_p$ is the two-body reduced mass, and $D(E)$ in Eq. (2) can be rewritten as a function of $k$ and expand near the threshold as power series of $k$, so-called the effective range expansion (ERE),

$$D(k) = \frac{1}{a} - ik + \frac{r_e}{2}k^2 + \mathcal{O}(k^3), \qquad (5)$$

where $a$ is the scattering length and $r_e$ is the effective range [31]. The $\mathcal{O}(k^3)$ term occurs due to the presence of charged channels. By doing so, the poles can be displayed in one plane, as shown in Fig. 2(c). The pole location on the upper half plane is $k^+ = (-12.6 + 12.3i)$ MeV, and that on the lower half plane is $k^- = (14.1–115.3i)$ MeV.

The statistical uncertainties of the pole locations, propagated from the line-shape parameters $g$, $\Gamma_0$, and $M_X$, are obtained by sampling the line-shape parameters according to their covariance matrix. Here, since the uncertainties are large, $g$ and $\Gamma_{\pi^+\pi^- J/\psi}$ could become negative in the $3\sigma$ confidence region, which exceeds the physical boundary. The events with negative $g$ or $\Gamma_{\pi^+\pi^- J/\psi}$ are dropped when calculating the statistical uncertainties of the pole locations (and other related parameters, as described as follows). The systematic uncertainties are obtained using the same treatment as that of the line-shape parameters. The detailed information of statistical and systematic uncertainties can be found in the Supplemental Material [24]. The pole locations including uncertainties are determined to be $E_{\mathrm{I}} = (7.04 \pm 0.15^{+0.07}_{-0.08}) + (-0.19 \pm 0.08^{+0.14}_{-0.19})i$ MeV and

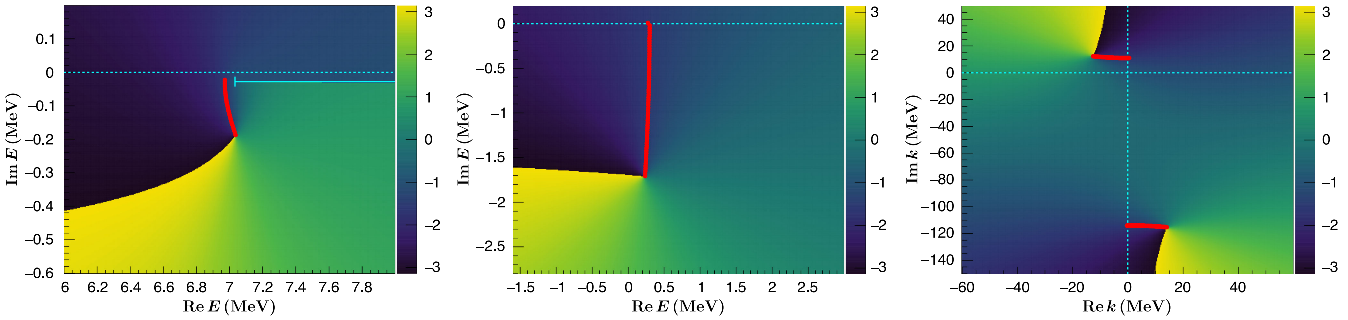

(a) Sheet I: $E_{\mathrm{I}} = 7.04 - 0.19i$ MeV

(b) Sheet II: $E_{\mathrm{II}} = 0.26 - 1.71i$ MeV

(c) $k$ plane: $k^+ = -12.6 + 12.3i$ MeV and $k^- = 14.1 - 115.3i$ MeV

FIG. 2. The phase of the amplitude on (a) Sheet I and (b) Sheet II with respect to complex energy. The solid cyan line starting from the point 7.033–0.027i MeV is the branch cut, the dashed cyan line is the real axis and the red trajectory approaching the real axis is obtained by continuously decreasing $\Gamma_0$ to 0. (c) The phase of the amplitude with respect to $k$. The upper (lower) half-plane corresponds to Sheet I (Sheet II).

$E_{\mathrm{II}} = (0.26 \pm 5.74^{+5.14}_{-38.32}) + (-1.71 \pm 0.90^{+0.60}_{-1.96})i$ MeV on the Riemann sheets, and $k^{+} = (-12.6 \pm 5.5^{+6.6}_{-6.2}) + (12.3 \pm 6.8^{+6.0}_{-6.4})i$ MeV and $k^{-} = (14.1 \pm 5.8^{+5.3}_{-2.1}) + (-115.3 \pm 44.6^{+52.7}_{-192.8})i$ MeV on the $k$ plane.

The relative ratio of the branching fractions of $\pi^{+}\pi^{-}J/\psi$ and $D^0\bar{D}^0\pi^0$ is determined to be $[\Gamma(\chi_{c1}(3872) \to \pi^{+}\pi^{-}J/\psi)/\Gamma(\chi_{c1}(3872) \to D^0\bar{D}^{*0})] = 0.05 \pm 0.01^{+0.01}_{-0.02}$, which is consistent with the global fit result $0.08 \pm 0.04$ [23] and 2020 BESIII result $0.08 \pm 0.02$ [19] within $1\sigma$, but lower than the value used as a Gaussian constraint in LHCb's work $0.11 \pm 0.03$ [17]. Compared to the previous result in Ref. [19], the ratio is smaller mainly due to the inclusion of the $D^{*+}D^{-}$ term in the model, which extends the tail of the line shape in the $D^0\bar{D}^0\pi^0$ channel and results in a larger signal yield.

We have estimated the ERE parameters, i.e., the scattering length $a$ and the effective range $r_e$ in Eq. (5). We consider a simplified case, according to the discussion in Ref. [32], by setting $\Gamma_0$ and $\Gamma_{D^*}$ to be 0. The amplitude contains the contribution from $D^*\bar{D}$ only with a stable $D^*$. After the simplification, the Eq. (5) can be used to extract ERE parameters, which are $a = (-16.5^{+7.0+5.6}_{-27.6-27.7})$ fm and $r_e = (-4.1^{+0.9+2.8}_{-3.3-4.4})$ fm.

Based on the obtained results, we can do a comparison between the $\chi_{c1}(3872)$ and the deuteron. The ERE parameters are related to the field renormalization constant $Z$ by

$$a = -\frac{2(1-Z)}{(2-Z)}\frac{1}{\gamma} + \mathcal{O}(\beta^{-1}), \tag{6}$$

$$r_e = -\frac{Z}{1-Z}\frac{1}{\gamma} + \mathcal{O}(\beta^{-1}), \tag{7}$$

where $\gamma = \sqrt{2\mu_p E_B}$, with $E_B$ the binding energy; the scale $\beta$ measures the momentum scale of the binding interaction, which cannot be calculated without knowing the details of the interaction, but can be estimated to be of the order of the pion mass $m_\pi$ for both neutron-proton and $D^*\bar{D}$ interactions, i.e., $1/\beta \sim 1/m_\pi \simeq 1.4$ fm.

In the limit of $Z \to 0$, the effective range should be positive and dominated by the range correction [32–35]. It was found that this case is compatible with the measured ERE parameters of the deuteron, which is known to be a predominantly molecular state [33]. However, in the case of the $\chi_{c1}(3872)$, we see that a negative effective range can fit the data well, which is different from the deuteron case ($+1.75$ fm) and also suggests an elementary component in the $\chi_{c1}(3872)$ [32]. Given that the range correction is less important in the case of the $\chi_{c1}(3872)$, one can solve Eqs. (6) and (7) for $Z$ by neglecting $\mathcal{O}(\beta^{-1})$, and obtain $Z = 0.18$. Besides, according to Ref. [34], $r_e$ is subject to the large correction from charged $D^*\bar{D}$ channel, after the subtraction of this charged contribution, $r_e$ becomes $-2.5$ fm and $Z$ becomes 0.12. However, in the case of the deuteron, it would be impossible to solve Eqs. (6) and (7) for $Z$ in a model independent way since the range correction term is non-negligible for $r_e$. Despite this, using the generalized compositeness $\tilde{X}_A$ proposed in Ref. [35], we find both the $\chi_{c1}(3872)$ and the deuteron have similar compositeness. Nevertheless, there are still large uncertainties in the ERE parameters, which prevent us from drawing strong conclusions on the nature of the $\chi_{c1}(3872)$. More statistics would be helpful.

In summary, we measure the line shape of the $\chi_{c1}(3872)$ by performing a simultaneous fit to the decay channels $D^0\bar{D}^0\pi^0$ and $\pi^{+}\pi^{-}J/\psi$. The line-shape parameters are determined to be $g = 0.16 \pm 0.10^{+1.12}_{-0.11}$, $\Gamma_0 = (2.67 \pm 1.77^{+8.01}_{-0.82})$ MeV, and $M_X = (3871.63 \pm 0.13^{+0.06}_{-0.05})$ MeV, where the first and second uncertainties are statistical and systematical, respectively. The FWHM of the line shape is determined to be $(0.44^{+0.13+0.38}_{-0.35-0.25})$ MeV.

BESIII Collaboration thanks the staff of BEPCII and the IHEP computing center for their strong support. This work is supported in part by National Key R&D Program of China under Contracts No. 2020YFA0406300, No. 2020YFA0406400; National Natural Science Foundation of China (NSFC) under Contracts No. 11635010, No. 11735014, No. 11835012, No. 11935015, No. 11935016, No. 11935018, No. 11961141012, No. 12022510, No. 12025502, No. 12035009, No. 12035013, No. 12061131003, No. 12192260, No. 12192261, No. 12192262, No. 12192263, No. 12192264, No. 12192265, No. 12221005, No. 12225509, No. 12235017; the Chinese Academy of Sciences (CAS) Large-Scale Scientific Facility Program; the CAS Center for Excellence in Particle Physics (CCEPP); Joint Large-Scale Scientific Facility Funds of the NSFC and CAS under Contract No. U1832207; CAS Key Research Program of Frontier Sciences under Contracts No. QYZDJ-SSW-SLH003, No. QYZDJ-SSW-SLH040; 100 Talents Program of CAS; The Institute of Nuclear and Particle Physics (INPAC) and Shanghai Key Laboratory for Particle Physics and Cosmology; ERC under Contract No. 758462; European Union's Horizon 2020 research and innovation programme under Marie Sklodowska-Curie grant agreement under Contract No. 894790; German Research Foundation DFG under Contracts No. 443159800, No. 455635585, Collaborative Research Center CRC 1044, FOR5327, GRK 2149; Istituto Nazionale di Fisica Nucleare, Italy; Ministry of Development of Turkey under Contract No. DPT2006K-120470; National Research Foundation of Korea under Contract No. NRF-2022R1A2C1092335; National Science and Technology fund of Mongolia; National Science Research and Innovation Fund (NSRF) via the Program Management Unit for Human Resources and Institutional Development, Research and Innovation of Thailand under

Contract No. B16F640076; Polish National Science Centre under Contract No. 2019/35/O/ST2/02907; The Swedish Research Council; U.S. Department of Energy under Contract No. DE-FG02-05ER41374.

[1] S. K. Choi *et al.* (Belle Collaboration), Phys. Rev. Lett. **91**, 262001 (2003).

[2] D. Acosta *et al.* (CDF Collaboration), Phys. Rev. Lett. **93**, 072001 (2004).

[3] V. M. Abazov *et al.* (D0 Collaboration), Phys. Rev. Lett. **93**, 162002 (2004).

[4] B. Aubert *et al.* (*BABAR* Collaboration), Phys. Rev. D **71**, 071103 (2005).

[5] R. Aaij *et al.* (LHCb Collaboration), Phys. Rev. D **92**, 011102 (2015).

[6] R. L. Workman *et al.* (Particle Data Group), Prog. Theor. Exp. Phys. **2022**, 083C01 (2022).

[7] K. Abe *et al.* (Belle Collaboration), arXiv:hep-ex/0505037.

[8] P. del Amo Sanchez *et al.* (*BABAR* Collaboration), Phys. Rev. D **82**, 011101 (2010).

[9] M. Ablikim *et al.* (BESIII Collaboration), Phys. Rev. Lett. **122**, 232002 (2019).

[10] E. S. Swanson, Phys. Lett. B **588**, 189 (2004).

[11] L. Zhao, L. Ma, and S.-L. Zhu, Phys. Rev. D **89**, 094026 (2014).

[12] L. Maiani, F. Piccinini, A. D. Polosa, and V. Riquer, Phys. Rev. D **71**, 014028 (2005).

[13] N. N. Achasov and E. V. Rogozina, Mod. Phys. Lett. A **30**, 1550181 (2015).

[14] M. Suzuki, Phys. Rev. D **72**, 114013 (2005).

[15] Y. S. Kalashnikova, Phys. Rev. D **72**, 034010 (2005).

[16] M. Takizawa and S. Takeuchi, Prog. Theor. Exp. Phys. **2013**, 093D01 (2013).

[17] R. Aaij *et al.* (LHCb Collaboration), Phys. Rev. D **102**, 092005 (2020).

[18] T. Aushev *et al.* (Belle Collaboration), Phys. Rev. D **81**, 031103 (2010).

[19] M. Ablikim *et al.* (BESIII Collaboration), Phys. Rev. Lett. **124**, 242001 (2020).

[20] M. Ablikim *et al.* (BESIII Collaboration), Chin. Phys. C **39**, 093001 (2015).

[21] M. Ablikim *et al.* (BESIII Collaboration), Chin. Phys. C **46**, 113002 (2022).

[22] C. Hanhart, Y. S. Kalashnikova, and A. V. Nefediev, Phys. Rev. D **81**, 094028 (2010).

[23] C. Li and C.-Z. Yuan, Phys. Rev. D **100**, 094003 (2019).

[24] See Supplemental Material at http://link.aps.org/supplemental/10.1103/PhysRevLett.132.151903 for details about line-shape parametrization, the determination of the mass resolution, and the uncertainties of the pole location.

[25] H. Albrecht *et al.*, Phys. Lett. B **241**, 278 (1990).

[26] J. L. Rosner, Phys. Rev. D **88**, 034034 (2013).

[27] M.-L. Du, V. Baru, X.-K. Dong, A. Filin, F.-K. Guo, C. Hanhart, A. Nefediev, J. Nieves, and Q. Wang, Phys. Rev. D **105**, 014024 (2022).

[28] C. Hanhart, Y. S. Kalashnikova, A. E. Kudryavtsev, and A. V. Nefediev, Phys. Rev. D **76**, 034007 (2007).

[29] M. Ablikim *et al.* (BESIII Collaboration), Chin. Phys. C **40**, 063001 (2016).

[30] P. Kowalczyk, IEEE Trans. Antennas Propag. **66**, 7198 (2018).

[31] T. Hyodo, Phys. Rev. Lett. **111**, 132002 (2013).

[32] A. Esposito, L. Maiani, A. Pilloni, A. D. Polosa, and V. Riquer, Phys. Rev. D **105**, L031503 (2022).

[33] S. Weinberg, Phys. Rev. **137**, B672 (1965).

[34] V. Baru, X.-K. Dong, M.-L. Du, A. Filin, F.-K. Guo, C. Hanhart, A. Nefediev, J. Nieves, and Q. Wang, Phys. Lett. B **833**, 137290 (2022).

[35] I. Matuschek, V. Baru, F.-K. Guo, and C. Hanhart, Eur. Phys. J. A **57**, 101 (2021).

M. Ablikim,[1] M. N. Achasov,[5,b] P. Adlarson,[75] X. C. Ai,[81] R. Aliberti,[36] A. Amoroso,[74a,74c] M. R. An,[40] Q. An,[71,58] Y. Bai,[57]
O. Bakina,[37] I. Balossino,[30a] Y. Ban,[47,g] V. Batozskaya,[1,45] K. Begzsuren,[33] N. Berger,[36] M. Berlowski,[45] M. Bertani,[29a]
D. Bettoni,[30a] F. Bianchi,[74a,74c] E. Bianco,[74a,74c] A. Bortone,[74a,74c] I. Boyko,[37] R. A. Briere,[6] A. Brueggemann,[68] H. Cai,[76]
X. Cai,[1,58] A. Calcaterra,[29a] G. F. Cao,[1,63] N. Cao,[1,63] S. A. Cetin,[62a] J. F. Chang,[1,58] T. T. Chang,[77] W. L. Chang,[1,63]
G. R. Che,[44] G. Chelkov,[37,a] C. Chen,[44] Chao Chen,[55] G. Chen,[1] H. S. Chen,[1,63] M. L. Chen,[1,58,63] S. J. Chen,[43] S. M. Chen,[61]
T. Chen,[1,63] X. R. Chen,[32,63] X. T. Chen,[1,63] Y. B. Chen,[1,58] Y. Q. Chen,[35] Z. J. Chen,[26,h] W. S. Cheng,[74c] S. K. Choi,[11]
X. Chu,[44] G. Cibinetto,[30a] S. C. Coen,[4] F. Cossio,[74c] J. J. Cui,[50] H. L. Dai,[1,58] J. P. Dai,[79] A. Dbeyssi,[19] R. E. de Boer,[4]
D. Dedovich,[37] Z. Y. Deng,[1] A. Denig,[36] I. Denysenko,[37] M. Destefanis,[74a,74c] F. De Mori,[74a,74c] B. Ding,[66,1] X. X. Ding,[47,g]
Y. Ding,[41] Y. Ding,[35] J. Dong,[1,58] L. Y. Dong,[1,63] M. Y. Dong,[1,58,63] X. Dong,[76] M. C. Du,[1] S. X. Du,[81] Z. H. Duan,[43]
P. Egorov,[37,a] Y. L. Fan,[76] J. Fang,[1,58] S. S. Fang,[1,63] W. X. Fang,[1] Y. Fang,[1] R. Farinelli,[30a] L. Fava,[74b,74c] F. Feldbauer,[4]
G. Felici,[29a] C. Q. Feng,[71,58] J. H. Feng,[59] K. Fischer,[69] M. Fritsch,[4] C. Fritzsch,[68] C. D. Fu,[1] J. L. Fu,[63] Y. W. Fu,[1] H. Gao,[63]
Y. N. Gao,[47,g] Yang Gao,[71,58] S. Garbolino,[74c] I. Garzia,[30a,30b] P. T. Ge,[76] Z. W. Ge,[43] C. Geng,[59] E. M. Gersabeck,[67]
A. Gilman,[69] K. Goetzen,[14] L. Gong,[41] W. X. Gong,[1,58] W. Gradl,[36] S. Gramigna,[30a,30b] M. Greco,[74a,74c] M. H. Gu,[1,58]
Y. T. Gu,[16] C. Y. Guan,[1,63] Z. L. Guan,[23] A. Q. Guo,[32,63] L. B. Guo,[42] M. J. Guo,[50] R. P. Guo,[49] Y. P. Guo,[13,f] A. Guskov,[37,a]
T. T. Han,[50] W. Y. Han,[40] X. Q. Hao,[20] F. A. Harris,[65] K. K. He,[55] K. L. He,[1,63] F. H. H. Heinsius,[4] C. H. Heinz,[36]
Y. K. Heng,[1,58,63] C. Herold,[60] T. Holtmann,[4] P. C. Hong,[13,f] G. Y. Hou,[1,63] X. T. Hou,[1,63] Y. R. Hou,[63] Z. L. Hou,[1]

H. M. Hu,[1,63] J. F. Hu,[56,i] T. Hu,[1,58,63] Y. Hu,[1] G. S. Huang,[71,58] K. X. Huang,[59] L. Q. Huang,[32,63] X. T. Huang,[50]
Y. P. Huang,[1] T. Hussain,[73] N. Hüsken,[28,36] W. Imoehl,[28] M. Irshad,[71,58] J. Jackson,[28] S. Jaeger,[4] S. Janchiv,[33] J. H. Jeong,[11]
Q. Ji,[1] Q. P. Ji,[20] X. B. Ji,[1,63] X. L. Ji,[1,58] Y. Y. Ji,[50] X. Q. Jia,[50] Z. K. Jia,[71,58] H. J. Jiang,[76] P. C. Jiang,[47,g] S. S. Jiang,[40]
T. J. Jiang,[17] X. S. Jiang,[1,58,63] Y. Jiang,[63] J. B. Jiao,[50] Z. Jiao,[24] S. Jin,[43] Y. Jin,[66] M. Q. Jing,[1,63] T. Johansson,[75] X. K.,[1]
S. Kabana,[34] N. Kalantar-Nayestanaki,[64] X. L. Kang,[10] X. S. Kang,[41] R. Kappert,[64] M. Kavatsyuk,[64] B. C. Ke,[81]
A. Khoukaz,[68] R. Kiuchi,[1] R. Kliemt,[14] O. B. Kolcu,[62a] B. Kopf,[4] M. Kuessner,[4] A. Kupsc,[45,75] W. Kühn,[38] J. J. Lane,[67]
P. Larin,[19] A. Lavania,[27] L. Lavezzi,[74a,74c] T. T. Lei,[71,k] Z. H. Lei,[71,58] H. Leithoff,[36] M. Lellmann,[36] T. Lenz,[36] C. Li,[48]
C. Li,[44] C. H. Li,[40] Cheng Li,[71,58] D. M. Li,[81] F. Li,[1,58] G. Li,[1] H. Li,[71,58] H. B. Li,[1,63] H. J. Li,[20] H. N. Li,[56,i] Hui Li,[44]
J. R. Li,[61] J. S. Li,[59] J. W. Li,[50] K. L. Li,[20] Ke Li,[1] L. J. Li,[1,63] L. K. Li,[1] Lei Li,[3] M. H. Li,[44] P. R. Li,[39,j,k] Q. X. Li,[50] S. X. Li,[13]
T. Li,[50] W. D. Li,[1,63] W. G. Li,[1] X. H. Li,[71,58] X. L. Li,[50] Xiaoyu Li,[1,63] Y. G. Li,[47,g] Z. J. Li,[59] Z. X. Li,[16] C. Liang,[43]
H. Liang,[1,63] H. Liang,[71,58] H. Liang,[35] Y. F. Liang,[54] Y. T. Liang,[32,63] G. R. Liao,[15] L. Z. Liao,[50] Y. P. Liao,[1,63] J. Libby,[27]
A. Limphirat,[60] D. X. Lin,[32,63] T. Lin,[1] B. J. Liu,[1] B. X. Liu,[76] C. Liu,[35] C. X. Liu,[1] F. H. Liu,[53] Fang Liu,[1] Feng Liu,[7]
G. M. Liu,[56,i] H. Liu,[39,j,k] H. B. Liu,[16] H. M. Liu,[1,63] Huanhuan Liu,[1] Huihui Liu,[22] J. B. Liu,[71,58] J. L. Liu,[72] J. Y. Liu,[1,63]
K. Liu,[1] K. Y. Liu,[41] Ke Liu,[23] L. Liu,[71,58] L. C. Liu,[44] Lu Liu,[44] M. H. Liu,[13,f] P. L. Liu,[1] Q. Liu,[63] S. B. Liu,[71,58] T. Liu,[13,f]
W. K. Liu,[44] W. M. Liu,[71,58] X. Liu,[39,j,k] Y. Liu,[81] Y. Liu,[39,j,k] Y. B. Liu,[44] Z. A. Liu,[1,58,63] Z. Q. Liu,[50] X. C. Lou,[1,58,63]
F. X. Lu,[59] H. J. Lu,[24] J. G. Lu,[1,58] X. L. Lu,[1] Y. Lu,[8] Y. P. Lu,[1,58] Z. H. Lu,[1,63] C. L. Luo,[42] M. X. Luo,[80] T. Luo,[13,f]
X. L. Luo,[1,58] X. R. Lyu,[63] Y. F. Lyu,[44] F. C. Ma,[41] H. L. Ma,[1] J. L. Ma,[1,63] L. L. Ma,[50] M. M. Ma,[1,63] Q. M. Ma,[1]
R. Q. Ma,[1,63] R. T. Ma,[63] X. Y. Ma,[1,58] Y. Ma,[47,g] Y. M. Ma,[32] F. E. Maas,[19] M. Maggiora,[74a,74c] S. Malde,[69] Q. A. Malik,[73]
A. Mangoni,[29b] Y. J. Mao,[47,g] Z. P. Mao,[1] S. Marcello,[74a,74c] Z. X. Meng,[66] J. G. Messchendorp,[14,64] G. Mezzadri,[30a]
H. Miao,[1,63] T. J. Min,[43] R. E. Mitchell,[28] X. H. Mo,[1,58,63] N. Yu. Muchnoi,[5,b] Y. Nefedov,[37] F. Nerling,[19,d] I. B. Nikolaev,[5,b]
Z. Ning,[1,58] S. Nisar,[12,l] Y. Niu,[50] S. L. Olsen,[63] Q. Ouyang,[1,58,63] S. Pacetti,[29b,29c] X. Pan,[55] Y. Pan,[57] A. Pathak,[35]
P. Patteri,[29a] Y. P. Pei,[71,58] M. Pelizaeus,[4] H. P. Peng,[71,58] K. Peters,[14,d] J. L. Ping,[42] R. G. Ping,[1,63] S. Plura,[36] S. Pogodin,[37]
V. Prasad,[34] F. Z. Qi,[1] H. Qi,[71,58] H. R. Qi,[61] M. Qi,[43] T. Y. Qi,[13,f] S. Qian,[1,58] W. B. Qian,[63] C. F. Qiao,[63] J. J. Qin,[72]
L. Q. Qin,[15] X. P. Qin,[13,f] X. S. Qin,[50] Z. H. Qin,[1,58] J. F. Qiu,[1] S. Q. Qu,[61] C. F. Redmer,[36] K. J. Ren,[40] A. Rivetti,[74c]
V. Rodin,[64] M. Rolo,[74c] G. Rong,[1,63] Ch. Rosner,[19] S. N. Ruan,[44] N. Salone,[45] A. Sarantsev,[37,c] Y. Schelhaas,[36]
K. Schoenning,[75] M. Scodeggio,[30a,30b] K. Y. Shan,[13,f] W. Shan,[25] X. Y. Shan,[71,58] J. F. Shangguan,[55] L. G. Shao,[1,63]
M. Shao,[71,58] C. P. Shen,[13,f] H. F. Shen,[1,63] W. H. Shen,[63] X. Y. Shen,[1,63] B. A. Shi,[63] H. C. Shi,[71,58] J. L. Shi,[13] J. Y. Shi,[1]
Q. Q. Shi,[55] R. S. Shi,[1,63] X. Shi,[1,58] J. J. Song,[20] T. Z. Song,[59] W. M. Song,[35,1] Y. J. Song,[13] Y. X. Song,[47,g] S. Sosio,[74a,74c]
S. Spataro,[74a,74c] F. Stieler,[36] Y. J. Su,[63] G. B. Sun,[76] G. X. Sun,[1] H. Sun,[63] H. K. Sun,[1] J. F. Sun,[20] K. Sun,[61] L. Sun,[76]
S. S. Sun,[1,63] T. Sun,[1,63] W. Y. Sun,[35] Y. Sun,[10] Y. J. Sun,[71,58] Y. Z. Sun,[1] Z. T. Sun,[50] Y. X. Tan,[71,58] C. J. Tang,[54] G. Y. Tang,[1]
J. Tang,[59] Y. A. Tang,[76] L. Y. Tao,[72] Q. T. Tao,[26,h] M. Tat,[69] J. X. Teng,[71,58] V. Thoren,[75] W. H. Tian,[52] W. H. Tian,[59]
Y. Tian,[32,63] Z. F. Tian,[76] I. Uman,[62b] S. J. Wang,[50] B. Wang,[1] B. L. Wang,[63] Bo Wang,[71,58] C. W. Wang,[43] D. Y. Wang,[47,g]
F. Wang,[72] H. J. Wang,[39,j,k] H. P. Wang,[1,63] J. P. Wang,[50] K. Wang,[1,58] L. L. Wang,[1] M. Wang,[50] Meng Wang,[1,63] S. Wang,[13,f]
S. Wang,[39,j,k] T. Wang,[13,f] T. J. Wang,[44] W. Wang,[72] W. Wang,[59] W. P. Wang,[71,58] X. Wang,[47,g] X. F. Wang,[39,j,k] X. J. Wang,[40]
X. L. Wang,[13,f] Y. Wang,[61] Y. D. Wang,[46] Y. F. Wang,[1,58,63] Y. H. Wang,[48] Y. N. Wang,[46] Y. Q. Wang,[1] Yaqian Wang,[18,1]
Yi Wang,[61] Z. Wang,[1,58] Z. L. Wang,[72] Z. Y. Wang,[1,63] Ziyi Wang,[63] D. Wei,[70] D. H. Wei,[15] F. Weidner,[68] S. P. Wen,[1]
C. W. Wenzel,[4] U. Wiedner,[4] G. Wilkinson,[69] M. Wolke,[75] L. Wollenberg,[4] C. Wu,[40] J. F. Wu,[1,63] L. H. Wu,[1] L. J. Wu,[1,63]
X. Wu,[13,f] X. H. Wu,[35] Y. Wu,[71] Y. J. Wu,[32] Z. Wu,[1,58] L. Xia,[71,58] X. M. Xian,[40] T. Xiang,[47,g] D. Xiao,[39,j,k] G. Y. Xiao,[43]
S. Y. Xiao,[1] Y. L. Xiao,[13,f] Z. J. Xiao,[42] C. Xie,[43] X. H. Xie,[47,g] Y. Xie,[50] Y. G. Xie,[1,58] Y. H. Xie,[7] Z. P. Xie,[71,58]
T. Y. Xing,[1,63] C. F. Xu,[1,63] C. J. Xu,[59] G. F. Xu,[1] H. Y. Xu,[66] Q. J. Xu,[17] Q. N. Xu,[31] W. Xu,[1,63] W. L. Xu,[66] X. P. Xu,[55]
Y. C. Xu,[78] Z. P. Xu,[43] Z. S. Xu,[63] F. Yan,[13,f] L. Yan,[13,f] W. B. Yan,[71,58] W. C. Yan,[81] X. Q. Yan,[1] H. J. Yang,[51,e] H. L. Yang,[35]
H. X. Yang,[1] Tao Yang,[1] Y. Yang,[13,f] Y. F. Yang,[44] Y. X. Yang,[1,63] Yifan Yang,[1,63] Z. W. Yang,[39,j,k] Z. P. Yao,[50] M. Ye,[1,58]
M. H. Ye,[9] J. H. Yin,[1] Z. Y. You,[59] B. X. Yu,[1,58,63] C. X. Yu,[44] G. Yu,[1,63] J. S. Yu,[26,h] T. Yu,[72] X. D. Yu,[47,g] C. Z. Yuan,[1,63]
L. Yuan,[2] S. C. Yuan,[1] X. Q. Yuan,[1] Y. Yuan,[1,63] Z. Y. Yuan,[59] C. X. Yue,[40] A. A. Zafar,[73] F. R. Zeng,[50] X. Zeng,[13,f]
Y. Zeng,[26,h] Y. J. Zeng,[1,63] X. Y. Zhai,[35] Y. C. Zhai,[50] Y. H. Zhan,[59] A. Q. Zhang,[1,63] B. L. Zhang,[1,63] B. X. Zhang,[1]
D. H. Zhang,[44] G. Y. Zhang,[20] H. Zhang,[71] H. H. Zhang,[59] H. H. Zhang,[35] H. Q. Zhang,[1,58,63] H. Y. Zhang,[1,58] J. J. Zhang,[52]
J. L. Zhang,[21] J. Q. Zhang,[42] J. W. Zhang,[1,58,63] J. X. Zhang,[39,j,k] J. Y. Zhang,[1] J. Z. Zhang,[1,63] Jianyu Zhang,[63]
Jiawei Zhang,[1,63] L. M. Zhang,[61] L. Q. Zhang,[59] Lei Zhang,[43] P. Zhang,[1] Q. Y. Zhang,[40,81] Shuihan Zhang,[1,63]
Shulei Zhang,[26,h] X. D. Zhang,[46] X. M. Zhang,[1] X. Y. Zhang,[50] Xuyan Zhang,[55] Y. Zhang,[72] Y. Zhang,[69] Y. T. Zhang,[81]

Y. H. Zhang,[1,58] Yan Zhang,[71,58] Yao Zhang,[1] Z. H. Zhang,[1] Z. L. Zhang,[35] Z. Y. Zhang,[44] Z. Y. Zhang,[76] G. Zhao,[1] J. Zhao,[40] J. Y. Zhao,[1,63] J. Z. Zhao,[1,58] Lei Zhao,[71,58] Ling Zhao,[1] M. G. Zhao,[44] S. J. Zhao,[81] Y. B. Zhao,[1,58] Y. X. Zhao,[32,63] Z. G. Zhao,[71,58] A. Zhemchugov,[37,a] B. Zheng,[72] J. P. Zheng,[1,58] W. J. Zheng,[1,63] Y. H. Zheng,[63] B. Zhong,[42] X. Zhong,[59] H. Zhou,[50] L. P. Zhou,[1,63] X. Zhou,[76] X. K. Zhou,[7] X. R. Zhou,[71,58] X. Y. Zhou,[40] Y. Z. Zhou,[13,f] J. Zhu,[44] K. Zhu,[1] K. J. Zhu,[1,58,63] L. Zhu,[35] L. X. Zhu,[63] S. H. Zhu,[70] S. Q. Zhu,[43] T. J. Zhu,[13,f] W. J. Zhu,[13,f] Y. C. Zhu,[71,58] Z. A. Zhu,[1,63] J. H. Zou,[1] and J. Zu[71,58]

(BESIII Collaboration)

[1]*Institute of High Energy Physics, Beijing 100049, People's Republic of China*
[2]*Beihang University, Beijing 100191, People's Republic of China*
[3]*Beijing Institute of Petrochemical Technology, Beijing 102617, People's Republic of China*
[4]*Bochum Ruhr-University, D-44780 Bochum, Germany*
[5]*Budker Institute of Nuclear Physics SB RAS (BINP), Novosibirsk 630090, Russia*
[6]*Carnegie Mellon University, Pittsburgh, Pennsylvania 15213, USA*
[7]*Central China Normal University, Wuhan 430079, People's Republic of China*
[8]*Central South University, Changsha 410083, People's Republic of China*
[9]*China Center of Advanced Science and Technology, Beijing 100190, People's Republic of China*
[10]*China University of Geosciences, Wuhan 430074, People's Republic of China*
[11]*Chung-Ang University, Seoul 06974, Republic of Korea*
[12]*COMSATS University Islamabad, Lahore Campus, Defence Road, Off Raiwind Road, 54000 Lahore, Pakistan*
[13]*Fudan University, Shanghai 200433, People's Republic of China*
[14]*GSI Helmholtzcentre for Heavy Ion Research GmbH, D-64291 Darmstadt, Germany*
[15]*Guangxi Normal University, Guilin 541004, People's Republic of China*
[16]*Guangxi University, Nanning 530004, People's Republic of China*
[17]*Hangzhou Normal University, Hangzhou 310036, People's Republic of China*
[18]*Hebei University, Baoding 071002, People's Republic of China*
[19]*Helmholtz Institute Mainz, Staudinger Weg 18, D-55099 Mainz, Germany*
[20]*Henan Normal University, Xinxiang 453007, People's Republic of China*
[21]*Henan University, Kaifeng 475004, People's Republic of China*
[22]*Henan University of Science and Technology, Luoyang 471003, People's Republic of China*
[23]*Henan University of Technology, Zhengzhou 450001, People's Republic of China*
[24]*Huangshan College, Huangshan 245000, People's Republic of China*
[25]*Hunan Normal University, Changsha 410081, People's Republic of China*
[26]*Hunan University, Changsha 410082, People's Republic of China*
[27]*Indian Institute of Technology Madras, Chennai 600036, India*
[28]*Indiana University, Bloomington, Indiana 47405, USA*
[29a]*INFN Laboratori Nazionali di Frascati, INFN Laboratori Nazionali di Frascati, I-00044 Frascati, Italy*
[29b]*INFN Sezione di Perugia, I-06100 Perugia, Italy*
[29c]*University of Perugia, I-06100 Perugia, Italy*
[30a]*INFN Sezione di Ferrara, INFN Sezione di Ferrara, I-44122 Ferrara, Italy*
[30b]*University of Ferrara, I-44122 Ferrara, Italy*
[31]*Inner Mongolia University, Hohhot 010021, People's Republic of China*
[32]*Institute of Modern Physics, Lanzhou 730000, People's Republic of China*
[33]*Institute of Physics and Technology, Peace Avenue 54B, Ulaanbaatar 13330, Mongolia*
[34]*Instituto de Alta Investigación, Universidad de Tarapacá, Casilla 7D, Arica 1000000, Chile*
[35]*Jilin University, Changchun 130012, People's Republic of China*
[36]*Johannes Gutenberg University of Mainz, Johann-Joachim-Becher-Weg 45, D-55099 Mainz, Germany*
[37]*Joint Institute for Nuclear Research, 141980 Dubna, Moscow region, Russia*
[38]*Justus-Liebig-Universitaet Giessen, II. Physikalisches Institut, Heinrich-Buff-Ring 16, D-35392 Giessen, Germany*
[39]*Lanzhou University, Lanzhou 730000, People's Republic of China*
[40]*Liaoning Normal University, Dalian 116029, People's Republic of China*
[41]*Liaoning University, Shenyang 110036, People's Republic of China*
[42]*Nanjing Normal University, Nanjing 210023, People's Republic of China*
[43]*Nanjing University, Nanjing 210093, People's Republic of China*
[44]*Nankai University, Tianjin 300071, People's Republic of China*
[45]*National Centre for Nuclear Research, Warsaw 02-093, Poland*

[46]*North China Electric Power University, Beijing 102206, People's Republic of China*
[47]*Peking University, Beijing 100871, People's Republic of China*
[48]*Qufu Normal University, Qufu 273165, People's Republic of China*
[49]*Shandong Normal University, Jinan 250014, People's Republic of China*
[50]*Shandong University, Jinan 250100, People's Republic of China*
[51]*Shanghai Jiao Tong University, Shanghai 200240, People's Republic of China*
[52]*Shanxi Normal University, Linfen 041004, People's Republic of China*
[53]*Shanxi University, Taiyuan 030006, People's Republic of China*
[54]*Sichuan University, Chengdu 610064, People's Republic of China*
[55]*Soochow University, Suzhou 215006, People's Republic of China*
[56]*South China Normal University, Guangzhou 510006, People's Republic of China*
[57]*Southeast University, Nanjing 211100, People's Republic of China*
[58]*State Key Laboratory of Particle Detection and Electronics, Beijing 100049, Hefei 230026, People's Republic of China*
[59]*Sun Yat-Sen University, Guangzhou 510275, People's Republic of China*
[60]*Suranaree University of Technology, University Avenue 111, Nakhon Ratchasima 30000, Thailand*
[61]*Tsinghua University, Beijing 100084, People's Republic of China*
[62a]*Turkish Accelerator Center Particle Factory Group, Istinye University, 34010 Istanbul, Turkey*
[62b]*Near East University, Nicosia, North Cyprus 99138, Mersin 10, Turkey*
[63]*University of Chinese Academy of Sciences, Beijing 100049, People's Republic of China*
[64]*University of Groningen, NL-9747 AA Groningen, The Netherlands*
[65]*University of Hawaii, Honolulu, Hawaii 96822, USA*
[66]*University of Jinan, Jinan 250022, People's Republic of China*
[67]*University of Manchester, Oxford Road, Manchester M13 9PL, United Kingdom*
[68]*University of Muenster, Wilhelm-Klemm-Strasse 9, 48149 Muenster, Germany*
[69]*University of Oxford, Keble Road, Oxford OX13RH, United Kingdom*
[70]*University of Science and Technology Liaoning, Anshan 114051, People's Republic of China*
[71]*University of Science and Technology of China, Hefei 230026, People's Republic of China*
[72]*University of South China, Hengyang 421001, People's Republic of China*
[73]*University of the Punjab, Lahore-54590, Pakistan*
[74a]*University of Turin and INFN, University of Turin, I-10125 Turin, Italy*
[74b]*University of Eastern Piedmont, I-15121 Alessandria, Italy*
[74c]*INFN, I-10125 Turin, Italy*
[75]*Uppsala University, Box 516, SE-75120 Uppsala, Sweden*
[76]*Wuhan University, Wuhan 430072, People's Republic of China*
[77]*Xinyang Normal University, Xinyang 464000, People's Republic of China*
[78]*Yantai University, Yantai 264005, People's Republic of China*
[79]*Yunnan University, Kunming 650500, People's Republic of China*
[80]*Zhejiang University, Hangzhou 310027, People's Republic of China*
[81]*Zhengzhou University, Zhengzhou 450001, People's Republic of China*

[a] Also at the Moscow Institute of Physics and Technology, Moscow 141700, Russia.

[b] Also at the Novosibirsk State University, Novosibirsk 630090, Russia.

[c] Also at the NRC "Kurchatov Institute", PNPI, 188300 Gatchina, Russia.

[d] Also at Goethe University Frankfurt, 60323 Frankfurt am Main, Germany.

[e] Also at Key Laboratory for Particle Physics, Astrophysics and Cosmology, Ministry of Education; Shanghai Key Laboratory for Particle Physics and Cosmology; Institute of Nuclear and Particle Physics, Shanghai 200240, People's Republic of China.

[f] Also at Key Laboratory of Nuclear Physics and Ion-beam Application (MOE) and Institute of Modern Physics, Fudan University, Shanghai 200443, People's Republic of China.

[g] Also at State Key Laboratory of Nuclear Physics and Technology, Peking University, Beijing 100871, People's Republic of China.

[h] Also at School of Physics and Electronics, Hunan University, Changsha 410082, China.

[i] Also at Guangdong Provincial Key Laboratory of Nuclear Science, Institute of Quantum Matter, South China Normal University, Guangzhou 510006, China.

[j] Also at Frontiers Science Center for Rare Isotopes, Lanzhou University, Lanzhou 730000, People's Republic of China.

[k] Also at Lanzhou Center for Theoretical Physics, Lanzhou University, Lanzhou 730000, People's Republic of China.

[l] Also at the Department of Mathematical Sciences, IBA, Karachi 75270, Pakistan.